

# The Effective Thermal Conductivity Method in Continuous Casting of Steel

**Pilvi Oksman, Shan Yu, Heli Kytönen, Seppo Louhenkilpi**

Department of Materials Science and Engineering, Aalto University,  
Vuorimiehentie 2, 02150 Espoo, Finland  
pilvi.oksman@aalto.fi; shan.yu@aalto.fi; heli.kytonen@aalto.fi;  
seppo.louhenkilpi@aalto.fi

---

*Abstract: The main concept of the effective thermal conductivity method is to include the effect of fluid flow in the heat transfer modelling by modifying the thermal conductivity of steel by a coefficient  $A$  to enhance the heat transfer in the liquid pool and the mushy zone in continuous casting. In this work, a case study comparison was conducted by calculating the actual flow field, heat transfer and solidification with a CFD model and comparing it with a model using the effective thermal conductivity method with  $A$  values ranging from 1 to 18. The objective of the study was to find out if the effective thermal conductivity can be used accurately to describe the effect of fluid flow and if so, which  $A$  values correspond to the CFD models results. The results indicate that the effective thermal conductivity method cannot be used reliably with constant  $A$  values: the best match in this study between the CFD model and the effective thermal conductivity method was with  $A$  value of 1 in the end of the strand and with values 9-18 in the mould area. It was concluded that main sources of inaccuracy in the effective thermal conductivity method were the use of constant  $A$  and the model's inability to take into account the increased heat transfer produced by the SEN. The authors suggest setting the coefficient  $A$  as a function of strand location in order to fix these inaccuracies in the effective thermal conductivity method for continuous casting of steel.*

*Keywords: continuous casting; effective thermal conductivity; steel; heat transfer; modelling*

---

## 1 Introduction and Background

The continuous casting of steel is a well-known process and 1468 million tonnes of steel were produced in 2012 by continuous casting globally [1]. In continuous casting, liquid steel is poured from the tundish to the submerged entry nozzle (SEN), from where it flows to the mould. The solidification process begins in the water-cooled mould, which is referred to as primary cooling. The strand is continuously pulled at casting speed  $u_c$ . The cooling process after the mould is referred to as secondary cooling. There the heat is removed from the strand by

conduction (roll contact), convection (water sprays or mist) and radiation (air). One of the key points of interest in continuous casting is the mushy zone, which is the area where liquid and solid exist at the same time and until the final solidification, the strand cannot be cut to the final dimensions. The mushy zone and its position are also important for the steel microstructure, soft reduction and defects.

Mizikar [2] introduced an approach for including the effect of convection (fluid flow) in 1967 in heat transfer modelling, which is known as the effective thermal conductivity method. In this method, instead of calculating the fluid flow with the so-called Navier-Stokes equations, the increased heat transfer by the liquid is calculated by modifying the thermal conductivity of steel. The thermal conductivity in the liquid pool and the mushy zone is increased by the factor  $A$ . When  $A$  has the value of 1, the heat transfer is not increased. The effective thermal conductivity method can be described for example with equation 1 [3, 4], where  $k_{eff}$  is the effective heat conductivity,  $f_s$  is the solid fraction and  $A$  is a constant ranging from 1 to 12 [2,3]. The formulation for the effective heat transfer (eqn.1) might be different between models, but the principle remains the same [3, 4].

$$k_{eff} = kf_s + Ak(1 - f_s) \quad (1)$$

Even though this method has been widely used in heat transfer modelling [2, 3, 5-12] of continuous casting of steel, only a few researchers [3, 5, 6, 8] have questioned its accuracy. The parameter  $A$  is often an arbitrary value and is fitted to obtain results that match the validation. Karlinski *et al.* [3] investigated the effect of the parameter  $A$  on the liquidus and solidus curves with values 1.5 and 5. They found that  $A$  has only a minor influence on the solidus temperature but a much more profound effect on the liquidus isotherm. [3] Mizikar [2] and Lait *et al.*[5] used the  $A$  value of 7 in their studies. They found that there was only a slight difference for solid shell thickness, although their research was limited only to the mould area. Szekely and Stanek [6] investigated the effect of the fluid flow pattern on the liquid pool by implementing a flow pattern on the liquid pool in addition to using Mizikar's [2] effective thermal conductivity approach. They found that the solidus is not affected by the flow pattern, but the superheat removal rate is markedly affected. [6] Choudhary *et al.*[8] investigated the heat transfer of a continuously cast low carbon steel billet and compared two approaches with the effective thermal conductivity: with effective thermal conductivity extending to the mushy zone as a function of the liquid fraction and with no effective thermal conductivity in the mushy zone. The differences were clearly shown in shell thickness and billet midface temperature. The midface temperature was reported to be approximately 4-5% lower with the 'mushy zone treatment'. Choudhary *et al.* [8] also compared results when the coefficient  $A$  was set to 1, 7, 12 and 30. The value of 30 showed no solidification in the mould, whereas raising the value from 1 to 7 affected the shell thickness only slightly.[8]

95.6% of world crude steel was produced with the continuous casting process in 2012 [1], which makes the thorough investigation of the process necessary. The main process phenomena are heat transfer, fluid flow and solidification. Because of the interconnected and complex nature of these phenomena, experimental studies concerning continuous casting are extremely challenging. This has led to the investigation of the system by numerical methods. The numerical methods are mainly aimed at process improvement and control. Heat transfer analysis by e.g. finite difference method is computationally efficient compared to solving coupled fluid flow, solidification and heat transfer, which enables the effective thermal conductivity method to be used in online control and observation. However, the method's accuracy is far from clear. This work has been conducted to determine if it's reasonable to use the effective thermal conductivity method for describing the effect of fluid flow and if so, which value of  $A$  to use. The method for this has been chosen to be a comparison between a coupled fluid flow model and the effective thermal conductivity method for heat transfer. The modelling comparison is well justified, because currently no experimental methods can be used to validate results inside the strand to the authors' knowledge. This model also includes the whole strand from meniscus to the end of the strand (here 25 m).

## 2 Methods

As concluded from previous work, it is currently unclear which value of coefficient  $A$  corresponds to the most realistic situation. The advancement in computer modelling has made it possible to model fluid flow, heat transfer and solidification simultaneously thereby making it possible to compare the effective thermal conductivity method with computations involving the calculation of the flow field via the Navier-Stokes equations. The aim of this study was to examine the correspondence of results between different  $A$  values and the model, which calculates the flow field in addition to heat transfer and solidification. Tempsimu-3D, an in-house code that uses the effective thermal conductivity method, was used to compute the steady-state heat transfer with different values of  $A$ . In Tempsimu-3D, the heat transfer is solved through equation 2:

$$\rho c_p \frac{\partial T}{\partial t} = \frac{\partial}{\partial x} \left( k \frac{\partial T}{\partial x} \right) + \frac{\partial}{\partial y} \left( k \frac{\partial T}{\partial y} \right) + \frac{\partial}{\partial z} \left( k \frac{\partial T}{\partial z} \right) + w \frac{\partial \rho c_p T}{\partial z} + S \quad (2)$$

where  $c_p$  is the specific heat capacity,  $k$  is the (effective) thermal conductivity which in this case is defined by equation 1,  $w$  is the velocity in casting direction using Cartesian coordinates  $(x, y, z)$ ,  $T$  is the temperature and  $S$  is a source term. Tempsimu-3D solves equation 2 by the enthalpy method, for details see [13]. A commercial CFD software package ANSYS Fluent version 14.0 was used to compute the flow field which included solidification and heat transfer (referred to

as the ‘CFD model’ from here on). The Navier-Stokes equations and the continuity condition for fluid flow modelling are shown in general form in equations 3-5 and equation 6 (continuity), where  $\rho$  is the density,  $u$ ,  $v$  and  $w$  are the velocities in Cartesian coordinates ( $x,y,z$ ),  $\mu$  is the viscosity and  $S_1$ ,  $S_2$  and  $S_3$  are source terms.

$$\rho \left( \frac{\partial u}{\partial t} + u \frac{\partial u}{\partial x} + v \frac{\partial u}{\partial y} + w \frac{\partial u}{\partial z} \right) = -\frac{\partial p}{\partial x} + \mu \left( \frac{\partial^2 u}{\partial x^2} + \frac{\partial^2 u}{\partial y^2} + \frac{\partial^2 u}{\partial z^2} \right) + \rho g_x + S_1 \quad (3)$$

$$\rho \left( \frac{\partial v}{\partial t} + u \frac{\partial v}{\partial x} + v \frac{\partial v}{\partial y} + w \frac{\partial v}{\partial z} \right) = -\frac{\partial p}{\partial y} + \mu \left( \frac{\partial^2 v}{\partial x^2} + \frac{\partial^2 v}{\partial y^2} + \frac{\partial^2 v}{\partial z^2} \right) + \rho g_y + S_2 \quad (4)$$

$$\rho \left( \frac{\partial w}{\partial t} + u \frac{\partial w}{\partial x} + v \frac{\partial w}{\partial y} + w \frac{\partial w}{\partial z} \right) = -\frac{\partial p}{\partial z} + \mu \left( \frac{\partial^2 w}{\partial x^2} + \frac{\partial^2 w}{\partial y^2} + \frac{\partial^2 w}{\partial z^2} \right) + \rho g_z + S_3 \quad (5)$$

$$\frac{\partial \rho}{\partial t} + \frac{\partial(\rho u)}{\partial x} + \frac{\partial(\rho v)}{\partial y} + \frac{\partial(\rho w)}{\partial z} = 0 \quad (6)$$

## 2.1 Domain Geometry

The simulations were done with geometry equivalent to a real-life bloom caster with dimensions 0.4 x 0.28 x 25 m. A significant difference between the models was the creation of a 40 x 40 mm inlet at the meniscus level in order to induce proper turbulence, since a SEN (or fluid flow) is not included in Tempsimu-3D. Even though this procedure brings differences between the models, it was considered vital with regard to carrying out more realistic caster modelling. The modelling domain was chosen to be 25 m from meniscus level, so that the outlet won't affect the simulation results in the fluid flow model and also to see the complete temperature and flow field extending to the final solidification point. Two-fold symmetry was utilized to reduce the computational domain.

## 2.2 Material Properties

The steel properties can be found in Table 1. The selected steel was a medium-carbon steel and the material properties were obtained from the IDS (InterDendritic Solidification)-model [14]. Two different steel densities ( $\rho_c$  and  $\rho_{liq}$ ) were used for the computations, because of the simplification of using a constant density to see if the CFD model produces matching results with Tempsimu-3D with a different density, i.e. a casting temperature density matches the Tempsimu-3D results with solidus temperature density. It was also assumed that the flow is incompressible and the effects of solidification shrinkage or mechanical stresses were not taken into account. Because a fixed grid is used and the shrinkage is not taken into account, the density must also be constant. Four cases were studied, Case1 referring to using the properties at casting temperature

and Case2 referring to using the steel properties at the solidus temperature. In a) cases, the specific heat capacity was a constant and in b) cases, it was a piecewise linear function.

Table 1  
Steel properties

Property	Symbol	Value	Unit
Liquidus temperature	$T_{liq}$	1780	K
Solidus temperature	$T_{sol}$	1718	K
Casting temperature	$T_c$	1825	K
Case1			
Steel density at $T_c$	$\rho_c$	6974	$\text{kg}\cdot\text{m}^{-3}$
Thermal conductivity at $T_c$	$k_c$	34	$\text{W}\cdot\text{m}^{-1}\text{K}^{-1}$
Viscosity at $T_c$	$\mu_c$	$5.4\cdot 10^{-3}$	$\text{kg}\cdot\text{m}^{-1}\text{s}^{-1}$
Specific heat capacity	$c_p$	a) constant at 825 b) a piece-wise linear function	$\text{J}\cdot\text{kg}^{-1}\text{K}^{-1}$
Case2			
Steel density at $T_{sol}$	$\rho_{sol}$	7320	$\text{kg}\cdot\text{m}^{-3}$
Thermal conductivity at $T_{sol}$	$k_{sol}$	33	$\text{W}\cdot\text{m}^{-1}\text{K}^{-1}$
Viscosity at $T_{sol}$	$\mu_{sol}$	$6.8\cdot 10^{-3}$	$\text{kg}\cdot\text{m}^{-1}\text{s}^{-1}$
Specific heat capacity	$c_p$	a) constant at 697 b) a piece-wise linear function	$\text{J}\cdot\text{kg}^{-1}\text{K}^{-1}$

### 2.3 Boundary Conditions and Computational Parameters

For the effective thermal conductivity method in Tempsimu-3D, the tested A values (ranging from 1 to 18) were based on values present in literature; 30 was considered to be too unrealistic a value [8]. In Tempsimu-3D, the flow field is fixed (casting speed) everywhere in the domain. The heat transfer boundary conditions provided by Tempsimu-3D match realistic caster conditions by including water sprays, air and roller contact. The mould heat flux in Tempsimu-3D also includes the effect of an air gap between the mould and the strand. For further details of Tempsimu-3D, the reader is referred to Reference 13. The heat transfer boundary conditions (BCs) were kept the same between Tempsimu-3D and ANSYS Fluent 14.0 by a user-defined function (udf), which reads the boundary conditions directly from Tempsimu-3D to Fluent. At the mould area, a heat flux boundary condition was used. Small discrepancies exist between the model boundary conditions, but the effect of differences was minimized by careful modifications. A mixed boundary condition for heat transfer was used below the mould. The mixed BC is presented in equation 7:

$$-k \frac{\partial T}{\partial n} = h_{eff} (T_{surf} - T_{ext1}) + \varepsilon \sigma (T_{surf}^4 - T_{ext2}^4) \quad (7)$$

where  $h_{eff}$  is the effective heat transfer coefficient,  $T_{surf}$  is the surface temperature,  $T_{ext}$  is the external temperature for cooling water or ambient temperature for radiation,  $\varepsilon$  is the emissivity and  $\sigma$  is the Stefan-Boltzmann constant. Accurate heat transfer conditions at the boundaries were considered a priority in the computation, as they have a lot of influence on the solidification phenomena.

The k- $\varepsilon$ -model was selected for the turbulence model because of its well-known behaviour. The solidification was executed with the enthalpy-porosity technique in Fluent. The approach includes treating the mushy zone as a porous medium with Darcy's law. Darcy's law is presented in general form in equation 8, where  $K$  is the permeability,  $\mu$  is the viscosity and  $p$  is the pressure. The damping induced by the mushy zone is added to the momentum and turbulence equations through the source terms (for momentum with  $S_1$  to  $S_3$  in equations 3-5). For further details on the used enthalpy-porosity technique, see ANSYS Fluent 14.0 manual [15].

$$\vec{u} = -\frac{K}{\mu} \nabla p \quad (8)$$

In both Case1 and Case2 the Reynolds numbers at the inlet were estimated using equation 9

$$Re = \frac{\rho u D_h}{\mu} \quad (9)$$

where Re is the Reynolds number,  $\rho$  is the density,  $D_h$  is the hydraulic diameter and  $\mu$  is the viscosity. The Reynolds numbers were both around 30000, which indicate that the conditions were clearly turbulent. The computational parameters for the CFD model can be found in Table 2. In Fluent, a 'mass flow inlet' adjusted to match the casting speed was used as inlet BC and 'pressure outlet' was used for the outlet. The wall boundaries were set as moving walls at casting speed. Pull velocity was set as casting speed in Fluent.

Table 2  
Computational parameters

Parameter	Symbol	Value	Unit
Mushy zone parameter	$A_{mush}$	10000	
Turbulent intensity	$I$	4.36 – 4.46	%
Hydraulic diameter	$D_h$	0.04	m
Casting speed	$u_c$	0.55	m·min <sup>-1</sup>

In addition, the values for turbulent kinetic energy  $k$  and the turbulence dissipation  $\varepsilon$  were determined through equations 10-12. Equation 10 determines the turbulent intensity  $I$  through the inlet Reynolds number. When estimating the turbulence intensity, the kinetic energy can be determined by equation 11, where  $u_{avg}$  is the mean velocity. As the turbulent kinetic energy and dissipation are interconnected, the turbulent dissipation can be determined by equation 12, where  $C\mu$  is an

experimental value, which is approximately 0.09 [15]). As seen from equations 10-12, the  $k$  and  $\varepsilon$  depend on values of  $C_\mu$ , Reynolds number at inlet  $Re_{D_h}$  and the length scale  $l$ . This accentuates that their values are only estimations, which affects the turbulence calculation and they should be chosen carefully.

$$I \equiv \frac{u'}{u_{avg}} = 0.16(Re_{D_h})^{-1/8} \quad (10)$$

$$k = \frac{3}{2} (u_{avg} I)^2 \quad (11)$$

$$\varepsilon = C_\mu^{3/4} \frac{k^{3/2}}{l} \quad (12)$$

Mesh independence was examined by using three different-sized meshes. The mesh sizes were: 87 500 cells, 700 000 cells and 2.8 million cells. Convergence criterion was the decrease in residuals by  $10^{-3}$ . With the 2.8 million cell mesh, convergence was judged when the energy residual had fallen by  $10^{-4}$  and the other residuals by  $10^{-3}$ . The computation was done in steady-state in order to save computation time.

## 2.4 Validation

The focus of this work is on the heat transfer and solidification. Differences between Tempsimu-3D and the CFD model were expected inside the strand, but good correlation was expected for the surface temperature profiles. Commonly, heat transfer is validated through pyrometer measurements [12, 16-19]. The validation of the CFD model here is accepted as a comparison to values of solid shell thickness and surface temperature profile(s) given by Tempsimu-3D, because set side by side with other heat transfer models, Tempsimu has been extensively validated. Previously, Tempsimu has been validated by pyrometer and solid shell thickness measurements in Finnish and Brazilian steel plants [20-23]. The solid shell thickness measurements were done with the 'wedge method'. An example of an excellent match between Tempsimu results and the solid shell thickness measurements can be seen in Figure 1, which proves that Tempsimu provides reliable data on the solidified shell thickness. In this case, it must be noted that the solid shell thickness measurements were only done for a limited distance, and don't prove exact accuracy (or validation) in the mould area or near the final solidification point. However, the mould boundary conditions in Tempsimu-3D have been fitted to match heat flux measurements from different casters. Further details of the validation and the 'wedge method' can be found in references [21, 23].

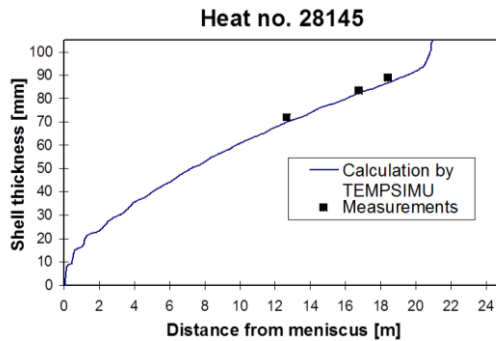


Figure 1

An excerpt from Tempsimu validations through solid shell thickness, from Ref. [21, 23]

In present work, the same comparison case of Ref. [21, 23] is not used for comparing the CFD model and Tempsimu, because the domain of the original comparison is much larger than the theoretical bloom calculated in this case by the CFD model. The use of a larger slab for example would take significantly more time to calculate because of the grid density requirements in order to obtain an accurate solution (See 3.1). In addition, the validation of the temperatures inside the liquid pool or in the mushy zone is currently impossible to the authors' knowledge. This is because of the extremely high temperatures in the liquid pool and the complexity of measuring temperatures from inside the mushy zone, which are serious challenges for measurement devices.

## 3 Results

### 3.1 Computational Factors

The liquid fraction at the centreline calculated by the CFD model with three different-sized meshes can be seen in Figure 2. It can be seen from Figure 2 that the liquid fraction changes significantly between the coarsest and the 700 000 cell mesh. The difference in liquid fraction becomes much smaller between the 700 000 and 2.8 million cell meshes and it was judged that mesh independence was reached. Several adjustments had to be made in the computational parameters of the CFD model in order to reach the convergence, which was also affected by the mesh quality. The computation time for the Tempsimu-3D model was considerably shorter than for the CFD model; the average computation time for Tempsimu-3D with the 2.8 million cell mesh was approximately 10 minutes with 3 Gb RAM PC and the CFD model computation time was several days with an 8 Gb RAM PC. The difference in computation time favours the use of the effective



thermal conductivity method and it should be noted that the modelling of a full-size slab would take approximately 11.2 million cells increasing the computation time significantly.

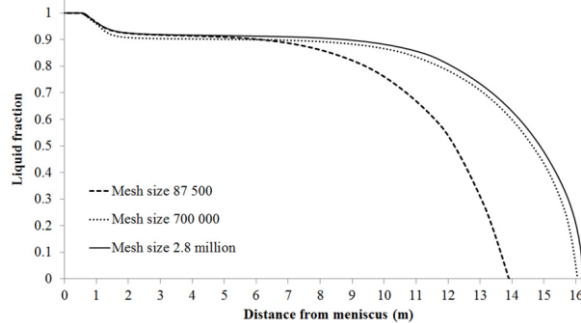


Figure 2

The calculated liquid fraction with the 87 500, 700 000 and 2.8 million cell meshes

### 3.2 The Effect of Fluid Flow in the CFD Model

The flow pattern itself was found to have no significant effect on the end position of the liquid pool in the strand. The effect of the flow pattern does not affect the solidification markedly near the final solidification point in this model, as the velocities approach the casting speed when nearing the final solidification point. However, the magnitude of the velocity does affect the final solidification point. Because the CFD model here is not sensitive enough to detect smaller scale phenomena, velocity or thermal gradients near the solid-liquid interphase could not be examined properly. The fluid flow pattern in the case was observed to be sufficiently symmetrical. The symmetry boundary condition could therefore be used to study the caster. In case of asymmetrical flow, the symmetry boundary condition cannot be used for x and y directions, because it would affect the forming flow pattern.

Because the calculated case is theoretical, the strong convection produced the partial melting of the solid shell in the mould. This makes the direct comparison of the liquidus and solidus curves fruitless, but qualitatively it can be said that the effect of fluid flow on the mould heat transfer is significant and changes the position of the liquidus curve markedly. The inlet implemented in the CFD model produces quite a difference between the models and further work must be conducted to obtain even more realistic fluid flow conditions in the vicinity of the mould instead of the theoretical approach used in this work.

### 3.3 Effect of the Material Properties

The core temperature is compared between Case1 a) and Case2 a) in Figure 3. It can be seen from Figure 3 that the most difference in core temperature appears at the end of the strand in all cases. The Tempsimu-3D cases are quite similar to each other, but the CFD model cases differ more between themselves, when the material properties are changed between Case1 and Case2.

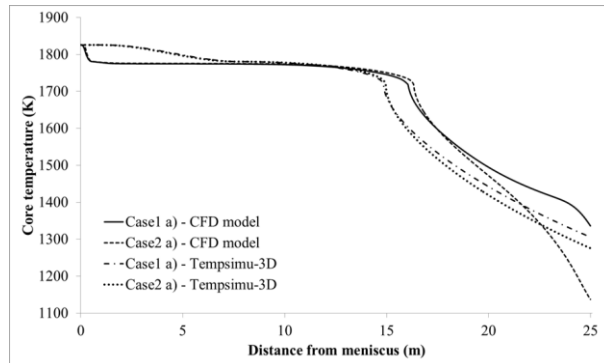


Figure 3

The comparison of core temperature between Cases 1 a) and 2 a)

The final point of solidification moved when a piecewise linear function was used for the specific heat capacity instead of a constant value. The final point of solidification in Case1 moved from 16.25 m to 15.28 m in the CFD model and from 14.86 m to 13.87 m in Tempsimu-3D between a) and b) cases. In both instances, the final solidification is affected by almost 1 m just by modifying the specific heat capacity. The difference in core temperature between Cases 1 a) and b) is shown in Figure 4. Based on Figure 4, it can be observed that even though there are understandable differences between the CFD model and the effective thermal conductivity model, there is a clear difference in using constant  $c_p$  and the effect of it is repeated in both models. The effect of using a constant  $c_p$  instead of a variable  $c_p$  produces a difference of approximately 74 degrees in Tempsimu-3D and 75 degrees in the CFD model at 20 m. This indicates clearly the importance of the material properties, because the difference presents itself in the same fashion in both of the models.

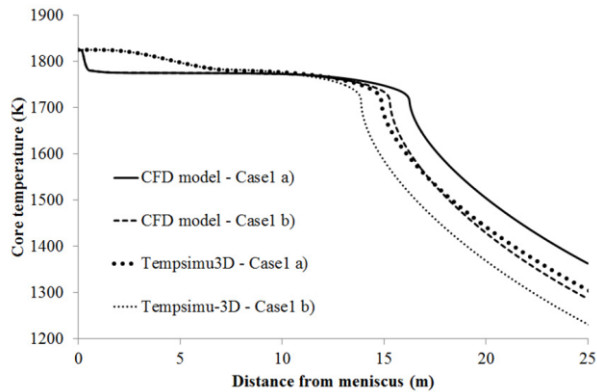


Figure 4

The comparison of core temperature between Case 1 a) and b)

### 3.4 The Effect of A on Temperature Profiles and Solid Shell Thickness

Because of the similarity in the behaviour of the Cases 1 and 2, Case 1 a) has been chosen as the example in Figures 5 and 6. The core temperature with different A values has been compared with the CFD model in Figure 5. It can be seen from Figure 5 that up until approximately 5 m from the meniscus the match between the CFD model and the effective thermal conductivity model with A values of 9 and 18 are closer than when A is 1. The situation is turned after 5 m distance from the meniscus, where it can be clearly seen that in core temperature, the A value of 1 is the closest match to the CFD model. Figure 6 shows the wide side ('x-direction') midface temperature, from which it can be observed that in the mould area and near it, the A value of 18 gives the most correspondence between the effective thermal conductivity method and the CFD model. The results for the narrow side midface temperature showed the same correlation. When nearing the end of the strand, it can be seen that the A value of 1 is a relatively good match to the CFD model compared with the larger A values. It can also be recognized from Figure 6 that the differences between models diminish the further the position from the meniscus, because the effect of the artificial inlet is reduced.

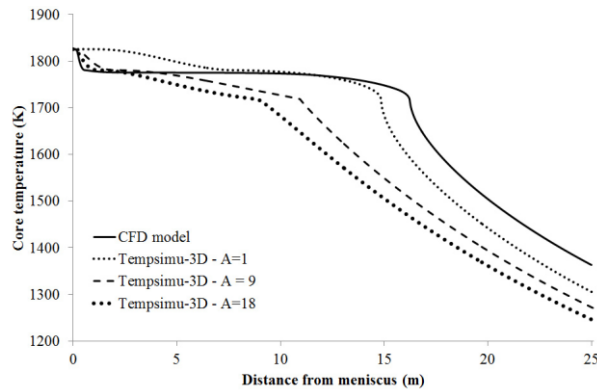


Figure 5

The core temperature comparison between the CFD model and different A values for Case1 a)

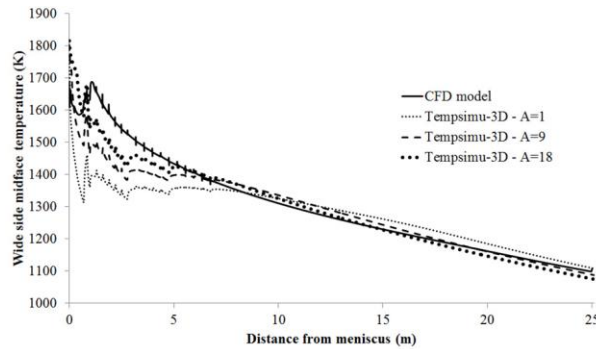


Figure 6

The wide side midface temperature comparison between the CFD model and different A values for Case1 a)

The comparison in solid shell thickness is shown in Figure 7, which clearly shows that the coefficient A should be a function of distance from meniscus: The value that closely matches the CFD model in the mould area and just below the mould is 18, whereas near the end of the domain, the A value should be even less than 1. The difference in the final solidification point can be explained through the actual calculation of the velocity field in the CFD model. As the velocities are calculated, more heat is transferred in the casting direction, because the velocities are higher than casting speed in certain parts of the strand. In the effective thermal conductivity method, constant casting speed is assumed in all locations of the strand, which means that the liquid transfers less hot liquid towards the final solidification point.

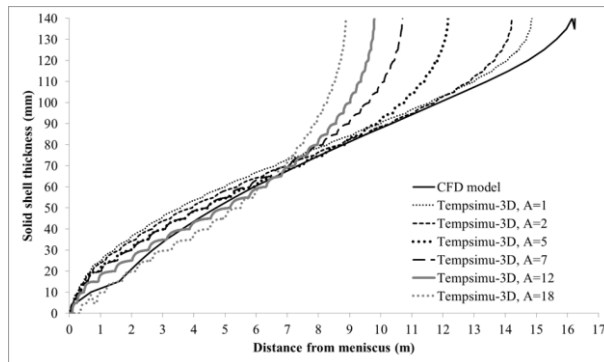


Figure 7

The comparison of solid shell thickness between the CFD model and different A values

## 4 Discussion

It was confirmed that the flow pattern in the liquid pool has no great effect on the solidification phenomena, as stated by Szekely and Stanek [6]. Especially near the final solidification point, the velocities were quite close to the casting speed so no effect could be found on the solidification front at this modelling scale. Because the effect of the flow pattern itself is small, the use of a full-scale CFD solidification model is only useful for academic purposes as the effective thermal conductivity method is much more computationally efficient. This underlines the need to develop an accurate heat transfer model, which can be used in industry to make real-time observations. For this purpose, the effective thermal conductivity method is superior to other heat transfer models, because the convection is taken into account as long as the parameter  $A$  is defined properly.

This work has been carried out to examine the use of the effective thermal conductivity method in continuous casting of steel. The method has been widely used over the years and its benefits are the ability to account for the fluid flow without arduous computations and the capability to suit many different casters with only small modifications. Each time a different caster is studied, in order to calculate fluid flow, solidification and heat transfer, a new model must be built into the software. This is time-consuming and it has many demands such as finding sufficient grid quality and choosing parameters. From this viewpoint, the effective thermal conductivity method is a good solution when searching for a fast and efficient model for online and control use. In this work, it has been shown that currently with constant  $A$  values, very reliable results cannot be obtained. The authors thereby suggest that  $A$  should be modified to match the CFD model's results more closely by setting the coefficient as a function of distance or position,

or as a function of cooling zones or in other similar methods. In this matter, the turbulent kinetic energy which describes the fluid flow conditions, shouldn't be used to observe the modifications of  $A$ , because the turbulent kinetic energy correlates with the heat transferred by turbulent phenomena. In the case of continuous casting, a prominent part of the heat is transferred by laminar fluid flow. The heat transfer effects of laminar fluid flow are more marked in the locations further away from the mould area, where the flow velocity decreases. Also, because the casters differ significantly in the positions of rolls, sprays etc., it would be extremely arduous to create a CFD model to obtain a new relation for  $A$  as a function of kinetic energy. The very purpose of this work is to show if it's possible to obtain reliable solidification and heat transfer results without computing the actual flow field every time.

The simplification of using a constant density and constant properties affects the results of the models. It was also observed that even the application of a piecewise linear specific heat capacity instead of a constant  $c_p$  affects the solidification significantly, which underlines the importance of the proper material data in continuous casting models.

Even the "theoretical" inlet had a large effect on the position of the liquidus isotherm, which implies that a real-life SEN would have an even greater effect. The absence of a SEN in the heat transfer model makes the effective thermal conductivity method unreliable in finding out the correct position of the mushy zone. This makes the use of the effective thermal conductivity method alone quite uncertain when considering actions that depend on the position of the mushy zone, such as soft reduction or electromagnetic stirring. This work shows that the effective thermal conductivity cannot be used reliably in caster optimisation concerning the mushy zone without further improvement to the factor  $A$ .

It was found that the  $A$  values of 9 and 18 match the CFD model results better in the mould area and until approximately until 5 m from meniscus. However, when approaching the end of the strand (from 5 m on), the correlation between the CFD model was the closest with  $A$  value of 1. This indicates clearly that the use of a constant  $A$  value is not appropriate for the length of the whole strand. Instead, the authors suggest that  $A$  should be a function of position, in effect varying between 1 and 18. As seen from Figures 5-7, it may be observed also that in effect the  $A$  could be closer to zero when coming closer to the end of the mushy zone. As the physical conditions of the fluid flow in the mushy zone depend on the forming solidification structures, a change should be observed where there is only the mushy zone and no free liquid pool flow.

Even though the validation of Tempsimu program has been extensive by literature standards, the solid shell thickness measurements were limited only to points several meters away from the final solidification point. There are differences in the results between the CFD model and Tempsimu-3D results especially in the beginning and end of the strand, which indicates that these points are the most

unreliable. It can be seen from Figure 7 that when the solid shell thickness is 60-70 mm that location is the least sensitive to different  $A$  values. It should be noted that the difference in liquid pool length in models can be due to the absence of a SEN in Tempsimu-3D because the flow from a straight SEN directs the flow towards the end at high velocity. The absence of the SEN also produces error in the effective thermal conductivity in the mould area because there the effect of flow is more noticeable.

## 5 Future Work

It has been established in this work that the effective thermal conductivity method cannot be reliably used in determining the position of the mushy zone or the inner temperature profiles near the SEN and in the mould area if constant  $A$  is used. It has also been established that the most convenient way to modify the method to be more accurate for different casters is to modify the coefficient  $A$  as a function of position (in the strand). However, because of the theoretical inlet used in this work, it is not reasonable to establish the best approach for  $A$  in this work. This is why a new industrial-based case has been initiated and is ongoing in the Metallurgy research group in Aalto University. The goal of the ongoing research is to study several different approaches for choosing  $A$  and compare the results to an industrial case study (and experiments). There are many possible ways to go about improving the effective thermal conductivity. Because currently it is quite unknown to establish how  $A$  is affected by for example electromagnetic stirring (EMS), one of the goals of future study is also to examine the effects of different SEN types and EMS.

### Conclusions

- (1) The effective thermal conductivity method was investigated using a commercial CFD model and a finite-difference-based heat transfer model Tempsimu-3D.
- (2) Different  $A$  values ranging from 1-18 were investigated to see which values give the best match between the effective thermal conductivity method and a full CFD model. It was found that in the mould area, the highest  $A$  values gave the best correlation between the models. However, in the end of the strand, the best match was given by values close to 1. This indicates clearly, that with constant  $A$  values, reliable values concerning the mushy zone and inner temperatures cannot be obtained through the whole length of strand.
- (3) It was concluded from the solid shell thickness comparison that  $A$  should be determined as a function of strand location or in similar fashion.

- (4) The constant material properties used in both models lead to significant differences in the results in comparison with non-constant properties and care should be taken to using proper material data.
- (5) The main cause for inaccuracy in the effective thermal conductivity in addition to the locality of the correct A value is the absence of a SEN, because the flow conditions have the most effect in the mould area.
- (6) It would be too arduous to continuously compute the flow field combined with solidification and heat transfer for different casters, which is why there is a strong motivation to develop the effective thermal conductivity method as it can be easily modified and used to examine the solidification and heat transfer including the effects of fluid flow. In further work different approaches for A will be investigated to find the best solution, based on an industrial case study.

### **Acknowledgement**

The authors would like to thank the Association of Finnish Steel and Metal Producers for funding of this work and CSC IT Center for Science Ltd for providing computational resources. The research was also partly carried out as a part of the Finnish Metals and Engineering Competence Cluster (FIMECC)'s ELEMET program.

### **References**

- [1] World Steel in Figures 2013. World Steel Association, Brussels, 2013
- [2] E. A. Mizikar: Mathematical Heat Transfer Model for Solidification of Continuously Cast Steel Slabs, Transactions of the Metallurgical Society of AIME, Vol. 239, 1967, pp. 1747-1753
- [3] V. Karlinski, S. Louhenkilpi, J. A. Spim: Accurate Modelling of Heat Transfer in Continuous Casting: Mathematical Formulas, Parameter Study and Effect of Steel Grade 40<sup>th</sup> Steelmaking Seminar International, Brazil, 2009
- [4] S. Louhenkilpi: Modelling of Heat Transfer in Continuous Casting, Materials Science Forum, Vol. 414-415, 2003, pp. 445-454
- [5] J. E. Lait, J. K. Brimacombe and F. Weinberg: Mathematical Modelling of Heat Flow in the Continuous Casting of Steel, Ironmaking & Steelmaking, 1974, No. 2, pp. 90-97
- [6] Szekely and V. Stanek: On Heat Transfer and Liquid Mixing in the Continuous Casting of Steel, Metallurgical Transactions, Vol. 1, Jan. 1970, pp. 119
- [7] J. C. Ma, Z. Xie, Y. Ci and G. L. Jia: Simulation and Application of Dynamic Heat Transfer Model for Improvement of Continuous Casting Process, Materials Science and Technology, Vol. 25, No. 5, 2009, pp. 636-639



- 
- [8] S. K. Choudhary, D. Mazumdar and A. Ghosh: Mathematical Modelling of Heat Transfer Phenomena in Continuous Casting of Steel, *ISIJ International*, Vol. 33, No.7, 1993, pp. 764-774
- [9] B. Lally, L. Biegler and H. Henein: Finite Difference Heat-Transfer Modelling for Continuous Casting, *Metallurgical Transactions B*, Vol. 21, 1990, 761-770
- [10] K.-H. Spitzer, K. Harste, B. Weber, P. Monheim and K. Schwerdtfeger: Mathematical Model for Thermal Tracking and On-Line Control in Continuous Casting, *ISIJ International*, Vol. 32, No. 7, 1992, 848-856
- [11] Y. Wang, D. Li, Y. Peng and L. Zhu: Computational Modelling and Control System of Continuous Casting Process, *International Journal of Advanced Manufacturing Technology*, Vol. 22, 2007, pp. 1-6
- [12] R. A. Hardin, K. Liu, A. Kapoor and C. Beckermann: A Transient Simulation and Dynamic Spray Cooling Control Model for Continuous Steel Casting, *Metallurgical and Materials Transactions B*, Vol. 34 2003, 297-306
- [13] S. Louhenkilpi, M. Mäkinen, S. Vapalahti, T. Räisänen and J. Laine: 3D Steady State and Transient Simulation Tools for Heat Transfer and Solidification in Continuous Casting, *Materials Science and Engineering*, Vol. 413-414, 2005, 135-138
- [14] J. Miettinen, S. Louhenkilpi, H. Kytönen and J. Laine: IDS: Thermodynamic–Kinetic–Empirical Tool for Modelling of Solidification, Microstructure and Material Properties, *Mathematics and Computers in Simulation*, Vol. 80, No. 7, 2010, pp. 1536-1550
- [15] ANSYS Inc. ANSYS Fluent Theory Guide, Release 14.0, Canonsburg (2011) USA
- [16] M. Shamsi and S. K. Ajmani: Three Dimensional Turbulent Fluid Flow and Heat Transfer Mathematical Model for the Analysis of a Continuous Slab Caster, *ISIJ International*, Vol. 47, No. 3, 2007, pp. 433-442
- [17] J. C. Ma, Z. Xie, Y. Ci and G. L. Jia: Simulation and Application of Dynamic Heat Transfer Model for Improvement of Continuous Casting Process, *Materials Science and Technology*, Vol. 25, No. 5, 2009, pp. 636-639
- [18] S. Chaudhuri, R. K. Singh, K. Patwari, S. Majumdar, A. K. Ray, A. K. P. Singh and N. Neogi: Design and Implementation of an Automated Secondary Cooling System for the Continuous Casting of Billets, *ISA Transactions*, Vol. 49, 2010, 121-129
- [19] C. A. Santos, E. L. Fortaleza, C. R. F. Ferreira, J. A. Spim and A. Garcia: A Solidification Heat Transfer Model and a Neural Network-based Algorithm Applied to the Continuous Casting of Steel Billets and Blooms, *Modelling*

- and Simulation in Materials Science and Engineering, Vol. 13, 2005, pp. 1071-1087
- [20] J. Miettinen, H. Kytönen, S. Louhenkilpi and J. Laine: IDS, TEMPSIMU, CASIM: Three Windows Applications for Continuous Casting of Steel, The 12<sup>th</sup> IAS Steelmaking Seminar, Instituto Argentino de Siderurgia, Buenos Aires, 1999, p. 488
- [21] H. Kytönen, M. Tolvanen, S. Louhenkilpi, L. Holappa: Experimental and Numerical Determination of Crater End in Continuous Casting of Steel, Modelling of Welding, Casting and Advanced Solidification Processes VIII, The Minerals, Metals & Materials Society, Warrendale, Pennsylvania 1998, p. 631
- [22] V. K. de Barcellos, C. R. Frick Ferreira, J. A. Spim and S. Louhenkilpi: Influence of Solidification Thermal Parameters on Columnar-to-equiaxed Transition in Continuous Casting of Steel Billets, CIM 2011 – VI Congreso Internacional del Materiales, Bogota, Colombia, 2011, pp. 1
- [23] H. Kytönen: Experimental and Numerical Determination of Crater end in Continuous Casting of Steel. Master's thesis, Helsinki University of Technology, Espoo 1997